Stem Cells Translational Medicine, 2022, **11**, 959–970
https://doi.org/10.1093/stcltm/szac045
Advance access publication 6 July 2022
Original Research

Lipidomics of Cell Secretome Combined with the Study of Selected Bioactive Lipids in an In Vitro Model of Osteoarthritis

Sara Casati[1,2,*], Chiara Giannasi[1,3], Stefania Niada[3], Elena Della Morte[3], Marica Orioli[1], Anna T. Brini[1,3]

[1]Dipartimento di Scienze Biomediche, Chirurgiche ed Odontoiatriche, Università degli Studi di Milano, Milan, Italy
[2]PhD Program in Experimental Medicine, Università degli Studi di Milano, Milan, Italy
[3]Laboratorio di Applicazioni Biotecnologiche, IRCCS Istituto Ortopedico Galeazzi, Milan, Italy

*Corresponding author: Sara Casati, Department of Biomedical, Surgical and Dental Sciences, Università degli Studi di Milano, Via Luigi Mangiagalli 37, 20133 Milan, Italy. Tel: +39 0250315648; Email: sara.casati@unimi.it

Abstract

Analytical advancements in lipidomics have enabled large-scale investigations of lipid biology. Herein, we focused on four bioactive lipid families, namely polyunsaturated fatty acids, eicosanoids, endocannabinoids, and N-acylethanolamines, and their involvement in the mesenchymal stem cells (MSC)-related inflammatory scenario. Since MSC secretome may represent a valid therapeutic alternative, here, the complete secretome and its vesicular component from adipose- and bone marrow-derived MSC and dermal fibroblasts were characterized by targeted mass spectrometry lipidomics. The 2-arachidonoylglycerol (2AG) and the palmitoylethanolamide (PEA), previously quantified in the MSC's secretome, were further investigated by assessing hypothetical effects in an in vitro model of osteoarthritis (OA) based on human primary articular chondrocytes (CH) stimulated with tumor necrosis factor alpha (TNFα). TNFα enhances the release of the inflammatory lipid prostaglandin E2 (PGE2), and an additional increment was observed when CH were treated with both TNFα and 2AG. In contrast, PEA downmodulates the PGE2 release to the levels of unstimulated CH suggesting a protective effect. TNFα also increases the expression of cyclooxygenase 2 (COX2), in particular when combined with 2AG, while PEA partly blunts TNFα-induced COX2 expression. In addition, TNFα-stimulated CH produce significantly higher levels of the inflammatory mediator nitric oxide (NO) both in the presence and in the absence of 2AG, and PEA was able to partially reduce NO release. Our results show a first partial lipidomic profile of MSC and DF secretome and suggest a possible implication of bioactive lipids in the OA scenario and in the future use of these cell-free products as innovative therapeutics.

Key words: secretome; lipids; mesenchymal stem cells; fibroblasts; eicosanoids; endocannabinoids

Graphical Abstract

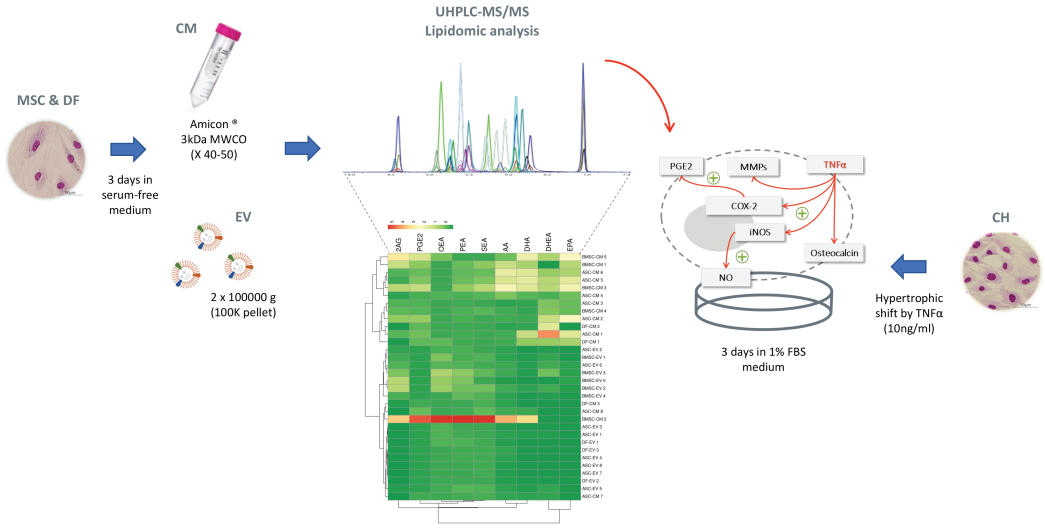

Lipidomic characterization of the complete cell secretome (CM) and the isolated extracellular vesicles (EV), derived from mesenchymal stem/stromal cells (MSC) and dermal fibroblasts (DF), followed by the evaluation of pro and anti-infllamatory effects of selected lipids in an vitro model of osteoarthritis (primary chondrocites – CH – treated with the tumor necrosis factor alpha – TNFα)

Received: 22 February 2022; Accepted: 14 May 2022.

Significance Statement

A solid understanding of the lipid individual bioactive factors secreted by mesenchymal stem/stromal cells and dermal fibroblasts and the mechanisms underlying their effect are indispensable to refine secretome-based therapies in several pathological processes, such as osteoarthritis.

Introduction

In the last decades, lipidomics has evolved rapidly due to its capability to offer new opportunities (ie, the advent of the next-generation mass spectrometry [MS]) for studying the roles of lipids in cellular biology as well as in health and disease.[1] Research focused in this field highlighted how the lipidome, as well as the transcriptome and the proteome, is in a dynamic balance and how changes in diet, physio-pathological conditions, and external stimuli can affect its homeostasis.[2,3] The diverse functions of lipids are highly dependent on their structures, their concentration, and their inter- and intracellular temporal and spatial distributions. Since 2005, lipids have been classified into eight main categories: (a) fatty acyls, (b) glycerolipids, (c) glycerophospholipids, (d) sphingolipids, (e) sterols, (f) prenol lipids, (g) saccharolipids, and (h) polyketides.[4] Further subclassifications, based on structural moieties and physiochemical features (eg, charge, polarity, size, shape, etc.) characterizing each of these eight lipid categories, have led to a total of 47 225 lipids in the LIPID MAPS Structure Database, among which 25 197 molecules are curated and 22 028 are computationally generated lipids (January 2022). If lipids are conventionally considered as structural components of cellular membranes, they have emerged recently as key players in a wide range of biological processes, such as signaling events and trafficking. However, their precise physio-pathological function is still poorly understood and a comprehensive characterization of lipids can provide pivotal information to better understand the roles exercised by these compounds in several biological phenomena. Based on their structure and biochemical functions, bioactive fatty acids and their derivatives can be grouped into different families: polyunsaturated fatty acids (PUFA), PUFA-derived molecules (known as eicosanoids), endocannabinoids (EC), and EC-related compounds N-acylethanolamines (NAE). The involvement of these bioactive lipids in the mesenchymal stem/stromal cells (MSC)-related inflammatory context was recently reviewed.[5] MSC are non-hematopoietic multipotent progenitor cells located in the perivascular area of most vessels throughout the body. Over the years, MSC have gained popularity as therapeutics in a variety of clinical scenarios thanks to their ability to promote tissue regeneration and reduce inflammation. Recently, growing evidence identifies the paracrine signaling as the main effector of MSC therapeutic action, overturning the initial hypothesis that acknowledged cell engraftment, differentiation, and replacement as the essential actors. The paracrine action is mediated by a broad array of secreted bioactive factors, collectively referred to as the whole secretome/conditioned medium (CM). The secretome is a mixture of soluble factors as well as molecules shuttled within extracellular vesicles (EV). EV are lipid bilayer delimited particles of various dimensions and complexities containing proteins, nucleic acids, and metabolites released into the extracellular space from cells and having both endosomal and plasma membrane origin.[6] Soluble components, such as nucleic acids, proteins, and lipids, can all be detected in the cell secretome, at different concentrations and activity levels depending on the cell type and environment.[7] In detail, the human MSC secretome contains both EV and a multitude of soluble molecules, including growth factors, cytokines, peptides, and hormones with a promising potential in regenerative medicine.[8] Up to now, lipid mediators are less well documented but have been described as bioactive factors released by human MSC.[9] Recently, in the context of cell therapy, also dermal fibroblasts (DF), the major cell type in the human dermis, have started to be considered a suitable alternative to MSC. Indeed, they share common characteristics including the same mesenchymal markers and multi-differentiative potential toward cells of the mesodermal lineage and, additionally, they exert anti-inflammatory, immunomodulatory, and regenerative actions.[10,11] Moreover, while the DF canonical therapeutic applications include skin regeneration and wound healing, our recent investigation has provided evidences of a pro-osteogenic effect of their secretome.[12] In recent years, our research focused on the characterization of the CM from adipose-derived mesenchymal stem/stromal cells (ASC) and DF in terms of both soluble factors and vesicular components, through different approaches (ie, Raman spectroscopy and proteomic analysis), highlighting substantial differences in the total lipid content and a clear distinction between the two derivatives, also considering inflammatory molecules.[13,14] For this reason, a solid understanding of the individual bioactive factors secreted by MSC and DF, including lipids, and the mechanisms underlying their effect are necessary to refine secretome-based therapies in several pathological processes, such as inflammation.[7,15,16] Moreover, we evaluated both ASC-CM and ASC-EV action in an in vitro model of human articular chondrocytes (CH) induced toward an osteoarthritis (OA)-like phenotype by the inflammatory cytokine tumor necrosis factor alpha (TNFα).[17,18] These previous studies proved that ASC-CM contains high levels of chondroprotective factors and exerts short-term anti-hypertrophic and anti-catabolic effects on TNFα-treated CH, confirming the beneficial action of these cell-free approaches in the management of OA. The present work aims at partially characterizing the lipid content of whole secretome and isolated EV, obtained from bone marrow-derived MSC (BMSC), ASC, and DF, using a targeted lipidomic MS approach.[19] Moreover, the role of two bioactive lipids—2-arachidonoylglycerol (2AG) and palmitoylethanolamide (PEA)—was assessed in the OA in vitro model.

Materials and Methods

Unless otherwise stated, reagents were purchased from Sigma-Aldrich, St. Louis, MO, USA.

Cell Cultures

Cell cultures were obtained from waste tissues collected at IRCCS Istituto Ortopedico Galeazzi upon Institutional

Review Board approval (procedure PQ7.5.125 Ver. 5). Every donor provided written informed consent. In detail, BMSC (2 males and 3 females, 64 ± 11 years old), ASC (8 females with no documented diagnosis of obesity, 44 ± 12 years old), DF (3 females, 46 ± 11 years old), and CH (3 males and 11 females, 67 ± 12 years old) were isolated from patients undergoing esthetic or prosthetic surgery, following well-established protocols.[12,17,20] In brief, BMSC isolation from bone marrow aspirate was performed by two centrifugation steps at 510*g* for 10 minutes. ASC were isolated by an enzymatic digestion of the fragmented subcutaneous adipose tissue with 0.75 mg/mL type I Collagenase (Worthington Biochemical Corporation, Lakewood, NJ, USA) for 30 minutes and filtering of the stromal vascular fraction through a 100-µm cell strainer (Corning Incorporated, Corning, NY, USA). DF were obtained by incubation of the fragmented dermis tissue with 1 mg/mL type I Collagenase (Worthington Biochemical Corporation, Lakewood, NJ, USA) until digestion and filtering with a 100-µm cell strainer (Corning Incorporated, Corning, NY, USA). CH derived from the femoral head of patients with OA who underwent total hip replacement: only the areas of macroscopically healthy cartilage (white, shiny, elastic, and firm) were harvested through a sterile scalpel and digested overnight at 37°C with 1.5 mg/mL type II Collagenase (Worthington Biochemical Corporation, Lakewood, NJ, USA). Cells were cultured in high glucose DMEM supplemented with 10% fetal bovine serum (FBS) (Euroclone, Pero, Italy), 2 mM L-glutamine, 50 U/mL penicillin, and 50 µg/mL streptomycin (complete DMEM [cDMEM]) at 37°C in a humidified atmosphere with 5% CO_2. The culture medium was further implemented with 110 µg/mL sodium pyruvate for CH maintenance.

CM and EV Production

ASC, BMSC, and DF from IV to XI passage at 90% of confluence were incubated in starving conditions for 72 hours (the absence of FBS). No signals of cell suffering were ever observed. The medium was collected and centrifuged at 2500*g* for 15 minutes at 4°C to remove dead cells, large apoptotic bodies, and debris. The supernatants were split in half to obtain paired CM and EV samples, while donor cells were counted in order to correlate cell number to the final products (CM or EV). An aliquot of the CM was concentrated about 40-50 times by centrifuging at 4000*g* for 90 minutes at 4°C in AmiconUltra-15 Centrifugal Filter Devices with 3 kDa molecular weight cutoff (Merck Millipore, Burlington, MA, USA). This procedure allows the retention of the vesicular component of cell secretome, as previously demonstrated in the studies of Carlomagno et al., Niada et al., and Giannasi et al.[13,14,18] In parallel, EV were isolated starting from CM through differential centrifugation at 100 000*g* (L7-65; Rotor 55.2 Ti; Beckman Coulter, Brea, CA, USA), 4°C for 70 minutes).[14,21] The resulting CM and EV were kept at −80°C until use.

Secretome Characterization by UHPLC-MS/MS-based Lipidomics

PUFA, eicosanoids, EC, and NAE were quantified on a Q Trap 5500 triple quadrupole linear ion trap mass spectrometer (Sciex, Darmstadt, Germany) coupled with an Agilent 1200 Infinity pump Ultra High-Pressure Liquid Chromatography (UHPLC) system (Agilent Technologies, Palo Alto, CA, USA) using the UHPLC-MS/MS methods previously reported.[19] Compounds were separated on a Kinetex UHPLC XB-C18 column (100 × 2.1 mm i.d, 2.6 p.s.) (Phenomenex, Torrance, CA, USA) using linear gradient elution of two solvents: 0.1% formic acid in water (mobile phase A) and methanol/acetonitrile (5:1; v/v) (mobile phase B). Briefly, CM (~200 µL/sample) and EV samples were spiked with deuterated internal standards, and 1 mL of cold acetonitrile was added for protein precipitation. After centrifugation, the supernatants were extracted with 4 mL of dichloromethane/isopropanol (8:2; v/v) and centrifuged again. The organic layer was separated, dried, and reconstituted in 60 µL methanol. 3 µL aliquot was analyzed for EC and NAE. The remaining solution was added with 500 µL hydrochloride acid (0.125 N) and 4 mL ethyl acetate/*n*-hexane (9:1; v/v). The organic phase was dried, and the residue was reconstituted in 60 µL acetonitrile. 25 µL aliquot of methanol obtained from the neutral extraction and 25 µL aliquot from acid extraction were merged and 10 µL were analyzed for PUFA and eicosanoids determination. Data acquisition and processing were performed using Analyst 1.6.2 and MultiQuant 2.1.1 Software (Sciex, Darmstadt, Germany), respectively.

In Vitro OA Induction and Treatments

CH were used at first culture passage in order to prevent their dedifferentiation.[22] CH were seeded at the density of 10^4 cells/cm^2 in tissue culture treated 6-well plates (Corning Incorporated, Corning, NY, USA) and cultured in cDMEM until the full confluence was reached,[23] then shifted in a complete medium containing 1% FBS and treated with 10 ng/mL TNFα for 3 days to mimic OA microenvironment,[17,24] without any media change. Concurrently, CH were treated with 1 pg/mL 2AG and 0.5 pg/mL PEA. CH culture media were collected and centrifuged for 5 minutes at 2000*g*, 4°C, to remove dead cells and debris and aliquoted. CH supernatants were stored at −20°C for further analyses.

Western Blotting of CH Samples

CH were lysed in 50 mM Tris-HCl (pH 7.5), 150 mM NaCl, 1% NP-40, and 0.1% SDS supplemented with protease inhibitor cocktail (PIC) and 2 mM phenylmethanesulfonylfluoride fluoride. Upon incubation on ice for 30 minutes, lysates were centrifuged for 15 minutes at 15 000*g*, 4°C. The protein content of each sample was quantified through BCA Assay (Thermo Fisher Scientific, Waltham, MA, USA). Samples were analyzed by 10% SDS-PAGE and Western blotting (WB), using standard protocols.[17] For each sample, 10 µg of protein extract were loaded and probed with the primary antibodies rabbit anti-COX2 (Cell Signaling, Danvers, MA, USA, 1:1000 diluted) and goat anti-GAPDH (Santa Cruz Biotechnology, 0.1 µg/µL, 1:1000 diluted). Specific bands were revealed upon incubation with appropriate secondary antibodies conjugated to horseradish peroxidase (Rabbit IgG Secondary antibody, Thermo Fisher Scientific, Waltham, MA, USA, dilution 1:10 000; Goat IgG Secondary Antibody, Santa Cruz Biotechnology, CA, USA; 0.1 µg/µL, 1:6000 diluted) followed by detection with ECL Westar Supernova (Cyanagen, Bologna, Italy). After image acquisition with ChemiDoc Imaging System, protein expression was quantified through Image Lab Software (Bio-Rad, Milan, Italy). To normalize target protein expression, the band intensity of each sample was divided by the intensity of the

loading control protein GAPDH. Then, the fold change was calculated by dividing the normalized expression from each lane by the normalized expression of the control sample (CTR = 1).

Nitric Oxide Determination in CH Supernatants

Nitric oxide (NO) was measured in CH culture media following the reduction of nitrates to nitrites using an improved Griess method (ab272517 Nitric Oxide Assay Kit, Abcam, Cambridge, Regno Unito). Absorbance was measured at 540 nm. Nitrites concentration was then determined from a nitrite standard curve (0-200 µM).

UHPLC-MS/MS Lipidomic Analysis of CH Supernatants

An aliquot of 500 µL CH supernatants was analyzed by UHPLC-MS/MS analysis for lipids determination using the above-described methods. The protein content of each cell lysate sample was quantified through BCA Assay (Thermo Fisher Scientific, Waltham, MA, USA). Measurements were performed in technical duplicates.

Data Analysis and Statistics

Statistical analysis was performed by one-way analysis of variance (ANOVA) followed by Tukey's post hoc test in case of normally distributed measures, otherwise by Friedman's test followed by Dunn's multiple comparison. P values <.05 were considered statistically significant. Data for BMSC, ASC, and DF secretome characterization are presented as box and whisker plots. The box represents the 25-75 interquartile range, and the horizontal line represents the median value. The whiskers represent the extreme values. Data relative to median and standard deviation values are presented in $\log_{10}$ of ng/mL or ng per million cells. All the analyses were performed using Prism 7 (GraphPad Software, La Jolla, CA, USA).

Results

Secretome Characterization

A targeted lipidomic analysis was applied to two preparations—CM (soluble factors and vesicular fraction included) and EV—deriving from BMSC, ASC, and DF to identify differentially secreted bioactive lipids. Up to now, the complex mixture of the secretome constituents, including lipids, has not been fully investigated, although its appropriate characterization is required in the perspective of a clinical use. A total of 32 lipids belonging to PUFA, eicosanoids, EC, and NAE were analyzed by MS techniques using the previously published analytical methods.[19] MS data were acquired for both CM and EV samples obtained from ASC (n = 8), BMSC (n = 5), and DF (n = 3). Primary cells and donor features are listed in Supplementary Table S1. Nine lipid molecules were identified and quantified in MSC- and DF-derived CM and EV samples. In detail, the presence of 2AG, PEA, oleoylethanolamide (OEA), stearoylethanolamide (SEA), docosahexaenoylethanolamine (DHEA) belonging to EC/NAE and arachidonic acid (AA), eicosapentaenoic acid (EPA), and docosahexaenoic acid (DHA) belonging to PUFA were reported in both preparations. Prostaglandin E2 (PGE2) was found only in CM samples. An enrichment in lipid content was displayed in almost all MSC-CM and DF-CM rather than paired MSC- and DF-derived EV. In particular, AA, EPA, DHA, and the n-acylethanolamide of DHA (DHEA) were found significantly increased in CM than their paired EV samples (Fig. 1). Mean values and 95% confidential interval were reported in Supplementary Table S2, while raw data in Supplementary Table S6. After a logarithmic transformation of lipids concentration levels found in CM and EV preparations to improve normality, all groups passed the Shapiro-Wilk test. The lipid content of BMSC, ASC, and DF groups were analyzed by a completely random ANOVA followed by Tukey's post hoc test. Measured lipids concentration for each group is shown in the box and whisker plots in Figs. 2 and 3 (raw data in Supplementary Table S6). Interestingly, the major differences were observed between BMSC and ASC/DF, suggesting similar lipid profile between ASC- and DF-derived secretome. Regarding CM samples, generally higher levels of lipids were found in BMSC (Figs. 2 and 3). 2AG and PGE2 levels were significantly different between BMSC and ASC, while PEA and SEA between BMSC and DF. Concerning EV, 2AG, PEA, and SEA were significantly different among BMSC-EV and both ASC-EV and DF-EV groups, but they did not differ between ASC-EV and DF-EV (Fig. 2). Moreover, a significant reduction was reported also for DHEA in DF-EV compared to BMSC-EV. In contrast, no significant differences were found for PUFA and eicosanoids between MSC- and DF-derived EV (Fig. 3). Finally, we performed unsupervised clustering and principal component analysis (PCA) to search for potential distinction between cell types and cell products based on all the 9 quantified lipids. No clear distinction was shown by clustering analysis (Supplementary Fig. S3). Differently, the PCA of BMSC and ASC samples suggested a higher degree of homogeneity in EV samples rather than CM preparations (Fig. 4).

Functional Role of Two Bioactive Lipids—2AG and PEA—in an In Vitro Model of OA

Considering MSC-CM future clinical translation and its promising anti-inflammatory therapeutic potential, we investigated the role of—2AG and PEA—detected in MSC-CM samples as 2 possible lipid actors in an in vitro model of OA. In detail, articular CH were stimulated with 10 ng/mL TNFα and treated with 1 pg/mL 2AG or 0.5 pg/mL PEA according to both the concentration quantified in the ASC-CM and the 1:5 recipient to donor cell ratio used in our previous studies.[18,25] The PGE2 release and the protein expression of COX2 were tested to investigate a possible effect of the two lipids on this pathway. As expected, TNFα significantly raised the extracellular concentration of the inflammatory mediator PGE2 (Fig. 5a). An additional increment was highlighted when CH were treated with the combination of TNFα and 2AG. In contrast, PEA showed a protective effect against the PGE2 release, providing a downmodulation up to the levels quantified in untreated CH. Accordingly, TNFα increased the expression of COX2 especially when in association with 2AG (Fig. 5b) and PEA (0.5 pg/mL) partly blunted the pro-inflammatory cytokine effect. Next, the levels of another key inflammatory mediator, namely NO, were assessed. Primary cultured CH produced low levels of NO, but the production of this mediator is strongly enhanced by 3 days of TNFα stimulation (Fig. 6), both alone or in combination with 2AG. PEA protective effect seemed to be confirmed with this marker, too. Indeed, this lipid partially counteracts TNFα-induced NO production.

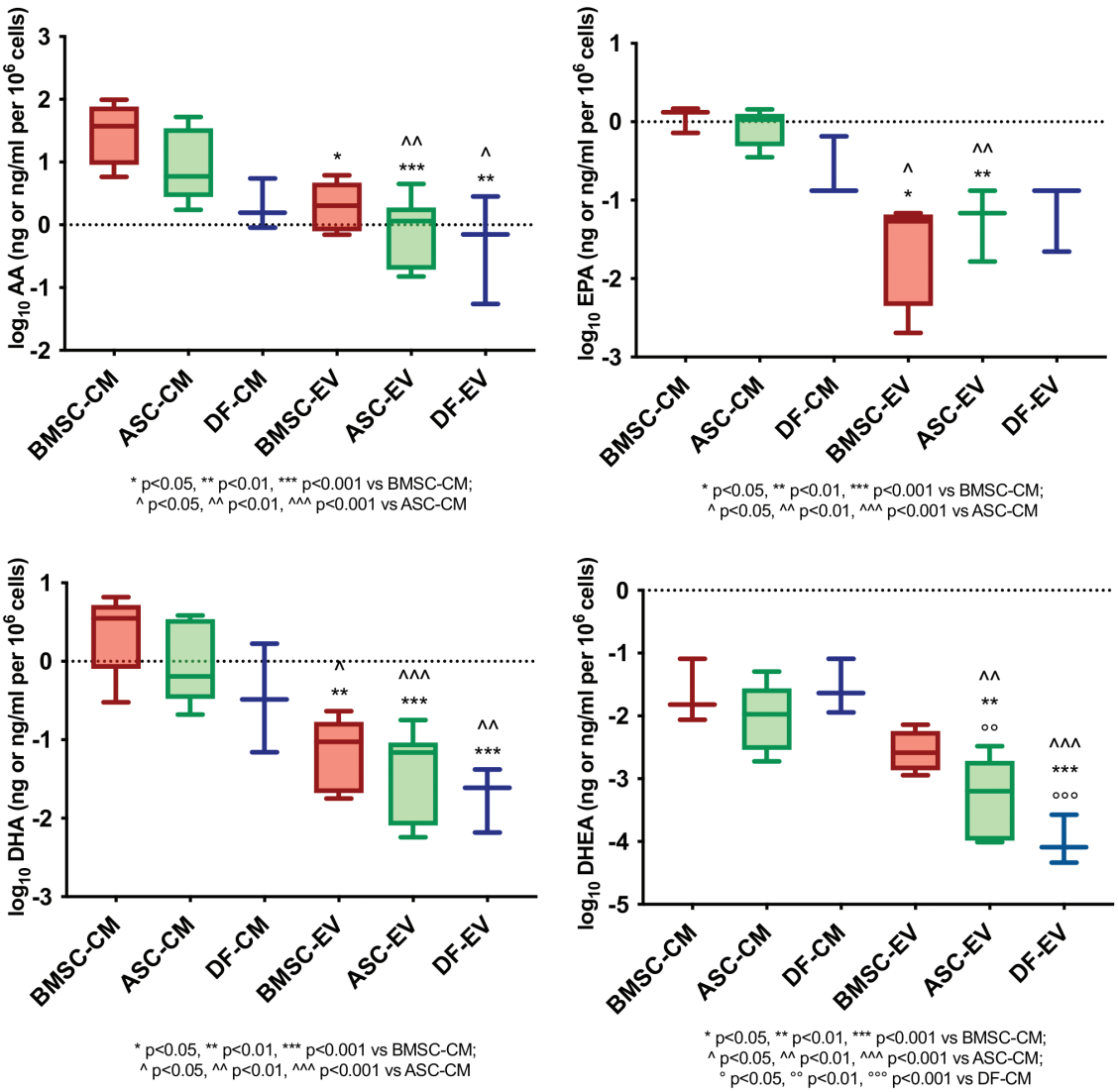

Figure 1. Box and whisker plots referred to AA, EPA, DHA, and DHEA levels in EV (log_{10} of ng per 10^6 cells) and CM (log_{10} of ng/mL per 10^6) cells from BMSC, ASC, and DF (ANOVA with Tukey's post hoc test; $P < .05$).

Modulation of PUFA Lipid Precursors and Bioactive Lipids in Untreated and TNFα-stimulated CH Cell Media

Considering a possible involvement of lipid precursors in inflammation and OA progression as well as the pivotal role of bioactive lipids (such as eicosanoids and EC/NAE), CH culture media were analyzed for 32 lipids by a previously developed UHPLC-MS/MS methods. At first, lipids were analyzed in the culture media of untreated as well as 2AG- and PEA-treated CH in the absence of TNFα. No significant differences were shown among treatments (Supplementary Fig. S4; Supplementary Table S7). However, unstimulated CH secrete low levels of PGE2, as previously reported, but also prostaglandin D2 (PGD2), prostaglandin F2 alpha (PGF2α), PEA, SEA, and DHEA were detected in the cell media of 2AG- and PEA-treated CH without TNFα. Differently, TNFα significantly decreases PUFA lipid precursors expression in CH culture media. Despite the inter-donor variability due to patient-derived articular CH, a clear effect of TNFα on PUFA expression was always determined, as shown in Fig. 7. AA, EPA, and DHA levels were significantly reduced by TNFα stimulation. Conversely, 2AG and PEA did not affect TNFα-reduced PUFA levels (Supplementary Fig. S5; Supplementary Table S8). No significant differences were displayed also for the further detected lipids by all considered TNFα treatments (Supplementary Fig. S5; Supplementary Table S8) with the only exception for PGE2 (Fig. 5).

Discussion

The therapeutic potential of the MSC secretome in diverse medical fields, from immunology to orthopedics, has been widely suggested by in vitro and in vivo evidences. In parallel, also DF might be also considered an alternative to MSC in the context of cell therapy. Nowadays, it is widely accepted that MSC action is largely mediated by paracrine mechanisms.[26] For this reason and due to the extreme complexity of their MSC-CM composition, a great multidisciplinary scientific effort to extensively characterize its composition is needed in the perspective of the future clinical translation. Our previous work[18] aimed at comparing the therapeutic effect of the

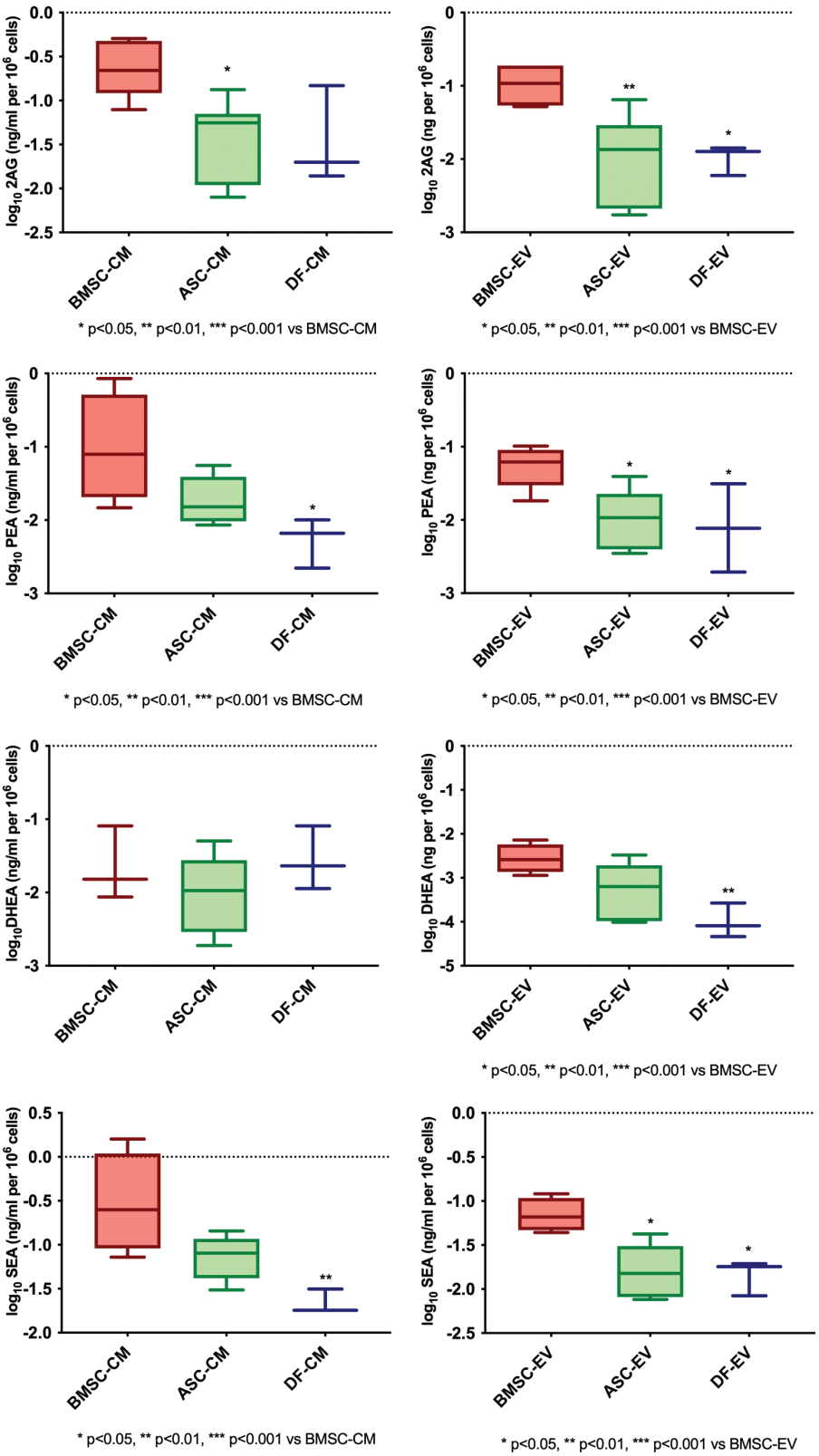

Figure 2. Box and whisker plots referred to EC and NAE levels in EV (log_{10} of ng per 10^6 cells) and CM (log_{10} of ng/mL per 10^6) from BMSC, ASC, and DF (ANOVA with Tukey's post hoc test; $P < .05$)., and

whole secretome and the EV in the OA context providing evidence of a higher therapeutic anti-OA potential of the first preparation compared to the latter. In particular, one of the most relevant differences was the greater reduction of the matrix metalloproteinases (MMPs) activity, correlated to the abundance of active tissue inhibitors of metalloproteinases (TIMPs) in ASC-CM. Moreover, ASC-CM appeared to be more abundant in cartilage protective factors and proteins

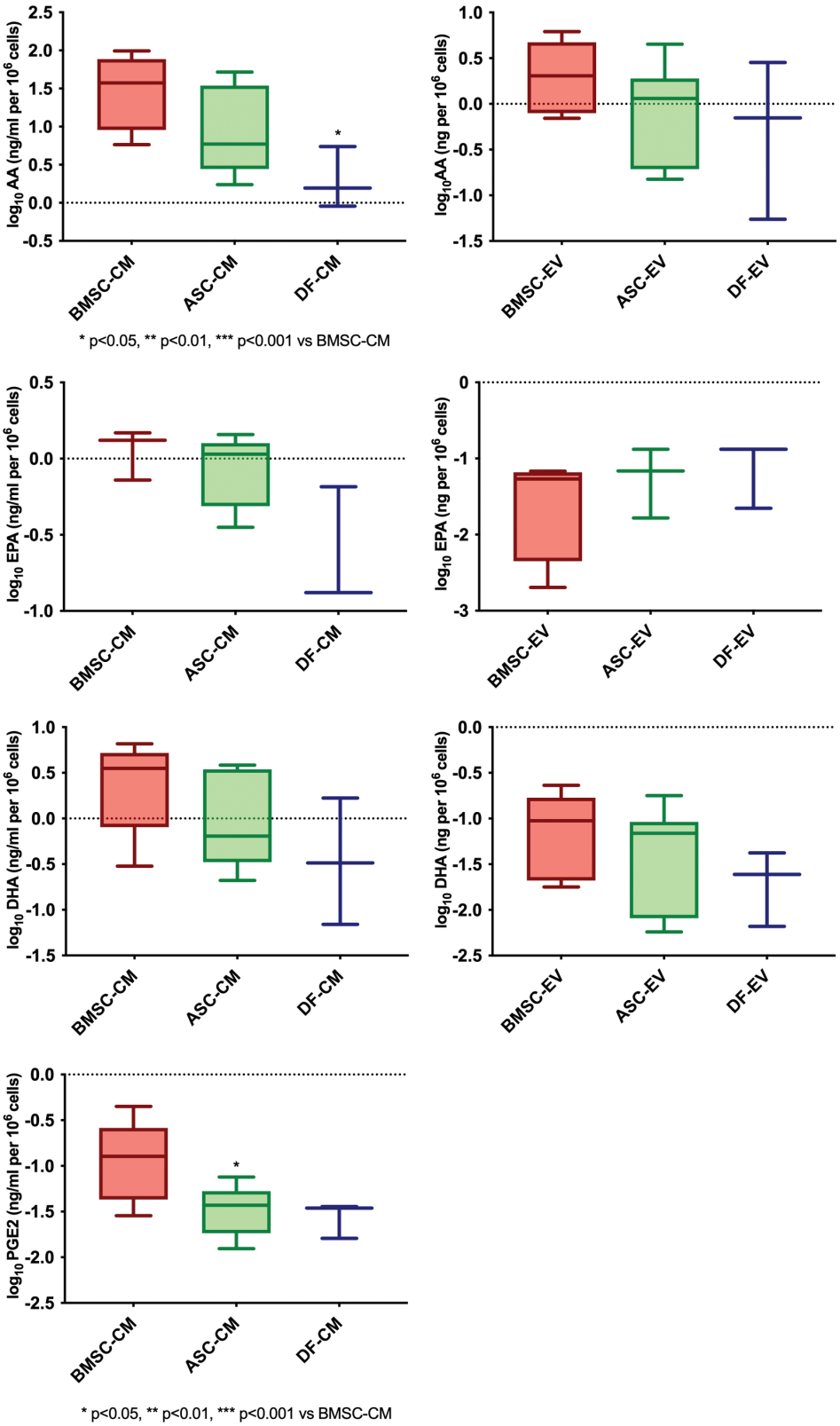

Figure 3. Box and whisker plots referred to PUFA and PGE2 levels in EV (log_{10} of ng per 10^6 cells) and CM (log_{10} of ng/mL per 10^6) from BMSC, ASC, and DF (ANOVA with Tukey's post hoc test; $P < .05$).

involved in ECM organization and chondrogenesis. Our recent research has identified key ingredients, including also lipids,[13] in ASC secretome that may be involved in its therapeutic action and whose consistent levels among different ASC-CM batches may represent promising quality control criteria.[27] In this work, our lipidomic MS developed methods[19] have demonstrated their usefulness in assessing a total of 9 lipid molecules in MSC- and DF-derived CM and EV

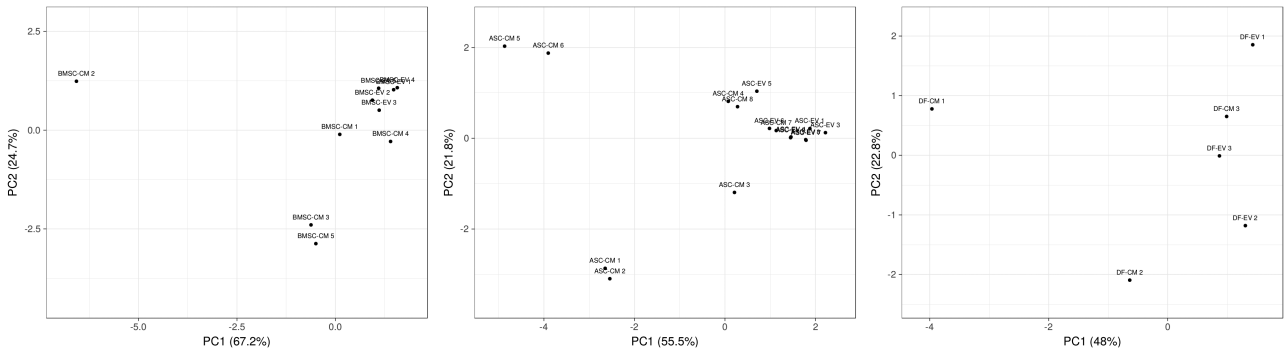

Figure 4. PCA on CM and EV lipid profiles of BMSC (a), ASC (b), and DF (c) from individual donors.

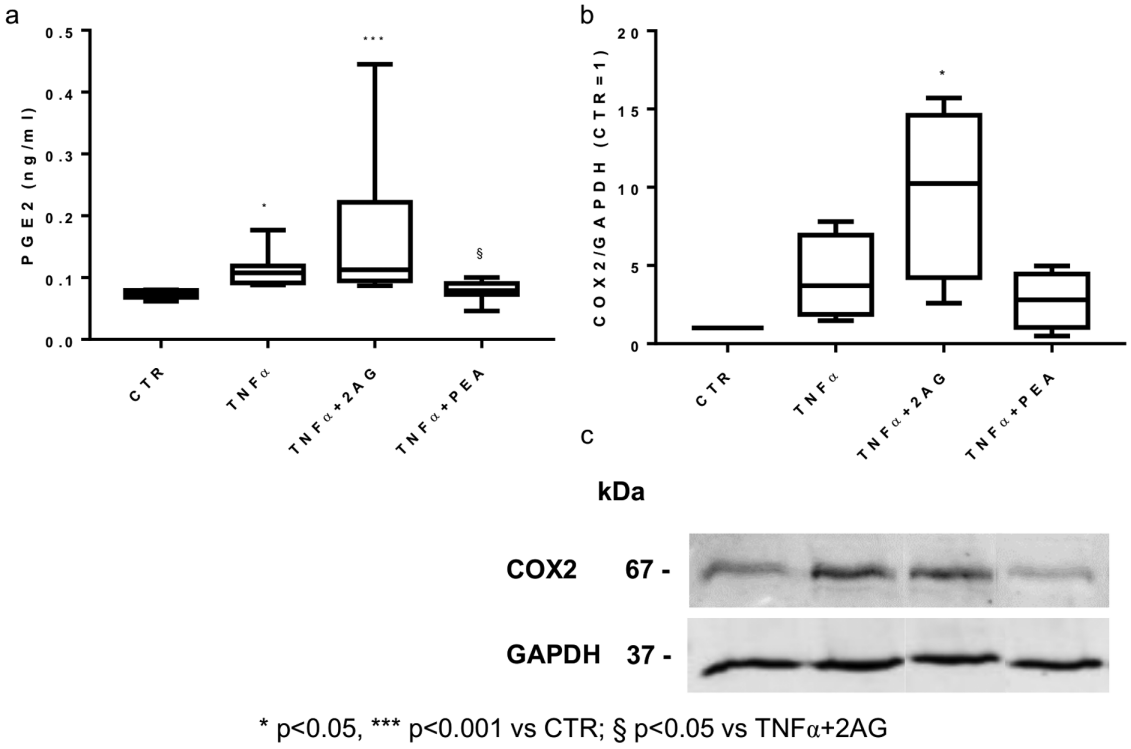

Figure 5. Modulation of PGE2 (a) and COX2 (b) by 2AG (1 pg/mL) and PEA (0.5 pg/mL). (a) PGE2 release, analyzed by UHPLC-MS/MS in CH culture medium (n = 8 independent experiments) for 3 days after treatments. (b) Quantification of the COX2 expression in TNFα-stimulated and 2AG- or PEA-treated CH at day 3 was analyzed by Western blotting. Data (n = 4 independent experiments) were normalized on GAPDH and expressed as relative values (CTR = 1). (c) Representative Western blots of COX2 expression by TNFα-stimulated and 2AG- or PEA-treated CH. GAPDH was used as internal control and COX2 densitometric evaluation was normalized on it.

samples. 2AG, PEA, OEA, SEA, DHEA belonging to EC/NAE and AA, EPA, DHA, PGE2 belonging to PUFA/eicosanoids were detected and quantified. Here we also showed that (i) CM samples are enriched in lipids compared to paired isolated EV, (ii) identified lipids in CM and EV can partially distinguish BMSC from ASC and DF, but not ASC from DF, and (iii) EV seem more homogeneous than CM preparations based on their lipid composition. An enrichment in lipid content was displayed in almost all MSC-CM and DF-CM rather than paired MSC- and DF-derived EV. This result appears in accordance with our previous work demonstrating a 3-4 times higher number of particles per million donor cells in CM preparations compared to EV ones.[13] These data could be explained by a suboptimal yield of the ultracentrifugation procedure, as already reported in the literature.[28,29] The PCA performed on BMSC-, ASC-, and DF-derived CM and EV samples suggested a higher homogeneity in EV than CM preparations for MSC only (Fig. 4). Regarding the differences between cell types, the major variations were observed in both BMSC-ASC and BMSC-DF comparisons, suggesting a more similar lipid profile between ASC- and DF-derived secretomes. Accordingly, differential proteomics and Raman spectroscopy on ASC and DF secretomes demonstrate that CM from these cell types share also common molecular patterns and composition profiles.[12,13] In order to confirm these data, we have recently performed an untargeted proteomic analysis (including hundreds of targets) to explore the protein composition of CM and EV from ASC and DF[14]: although differences were displayed for multiple factors, some biological processes were shared between ASC- and DF-derived products. Finally, the levels of the inflammatory mediator PGE2 were found significantly lower in ASC-CM than BMSC-CM. This PG is

generally known to exert multiple opposed functions based on its concentration, thus its quantification in CM could be remarkable in several pathological and inflammatory contexts.

In the last years, the safety and the efficacy of MSC in counteracting OA have been proved, as well as the MSC-CM therapeutic action on cartilage, subchondral bone, and synovium.[30,31] In this context, CM represents a promising complete product characterized by an easier manufacturing procedure and a minor manipulation, accounting for a more feasible scale up, in comparison to ultracentrifuge-isolated EV. Additionally, ASC-CM preparations obtained through the filtration of the culture medium allow also a complete retention of the vesicular component.[17,32] Considering future clinical applications in the OA management and the previous promising results obtained in OA context by ASC-CM treatment, we investigated the potential role of two bioactive lipids, at the concentrations quantified in ASC-CM, 2AG and PEA (whose action is widely documented in other inflammatory diseases,[33,34] in an in vitro model of OA. Indeed, the role of some lipid mediators, including fatty acids, sphingolipids, EC, and eicosanoids is increasingly recognized in the regulation of OA-related pathophysiological processes, including joint metabolism and pain.[35,36] Recent studies support the involvement of n-3 PUFA (ie, EPA and DHA) and their anti-inflammatory and pro-resolving derivatives in OA.[37] These lipids were identified in the OA joint and showed beneficial effects on cartilage health in vitro and reduced pain in animal models and patients with OA.[38,39] Moreover, also the EC system and its mediators, ie, NAE (14:2) and NAE (16:2),[36] are involved in the manifestation of OA-related pain and inflammation.[40,41] Here, all data were assessed after 3 days of treatments, since previous studies conducted by our laboratory revealed a beneficial action of ASC-CM at the same time point, including anti-inflammatory properties, in the OA context.[18,25] An opposite modulation of inflammatory factors (ie, PGE2 and COX2) by 2AG and PEA was reported in TNFα-treated CH. Our data confirm a PGE2 extracellular concentration enhancement by 10 ng/mL TNFα treatment (Fig. 5a). We have previously demonstrated a possible counteracting effect of ASC-CM in decreasing PGE2 upregulation.[18] Here, an additional increment in PGE2 content was highlighted when CH were treated with the combination of TNFα and 2AG. In contrast, PEA reduced the PGE2 production, providing a downmodulation up to 0.08 ± 0.02 ng/mL and restoring its physiological levels linked to a healthy CH phenotype (0.07 ± 0.01 ng/mL). Gabrielsson et al. proposed a linkage between reduced levels of PG and the blockage of hydrolysis of PEA to palmitic acid.[42] Generally, unstimulated CH release low amounts of PGE2 that are consistent with the concentrations known to inhibit collagen cleavage and the expression of hypertrophy markers.[43]

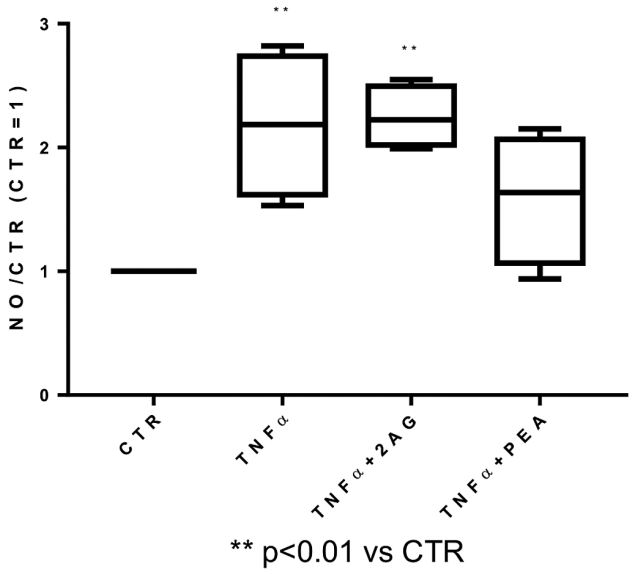

Figure 6. Quantification of NO by 2AG (1 pg/mL) and PEA (0.5 pg/mL) treatments NO production, analyzed in CH culture medium ($n = 4$ independent experiments) at day 3, is expressed as [nitrite] μM. Data were expressed as relative values (CTR = 1).

It is known that TNFα treatment induces PGE2 release through the activation of COX2 transcription via nuclear factor kappa-light-chain-enhancer of activated B cells (NF-κB).[44] Also, in this context, TNFα increased the expression of COX2 especially when in association with 2AG, suggesting a possible interconnection (Fig. 5b). In contrast, PEA partly blunts TNFα effect on the production of COX2. The ability of PEA to reduce COX2 expression and/or PG release was determined in other in vivo studies using models of pain and/or inflammation,[45-47] while a reduction in COX2 activity was observed in a macrophage cell line, but without a direct effect of PEA on COX2 levels.[42]

Moreover, it is well known that inflamed CH produce large quantities of NO by inducible nitric oxide synthase (iNOS), for example when stimulated by inflammatory cytokines (ie, interleukin-1 [IL-1]) or lipopolysaccharide (LPS).[48] Also, cartilage obtained from patients with arthritis produces

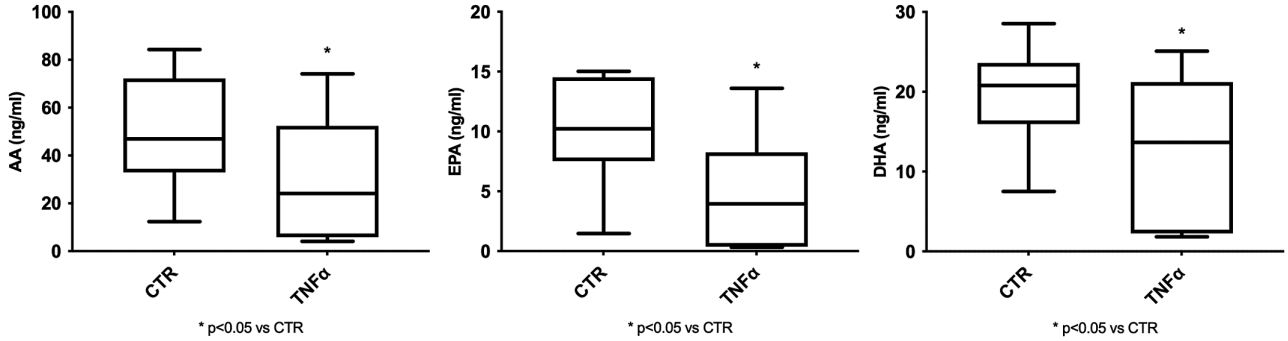

Figure 7. Quantification of AA, EPA, and DHA in TNFα-stimulated CH cell media at day 3 was analyzed by UHPLC-MS/MS analysis. Data ($n = 9$ independent experiments) were expressed in ng/mL (Student t test; $P < .05$).

significant amounts of NO ex vivo, even in the absence of IL-1 or LPS.[48] NO has been shown to be a key inflammatory mediator in tissue injury in a variety of pathological conditions and there are increasing evidences that excessive NO production could be a pivotal factor in the early stages of OA.[49-51] Here, while unstimulated CH produce low levels of NO, its release is strongly enhanced by the TNFα inflammatory stimulus. This could be at least partially responsible for the downstream negative effects mediated by TNFα. Indeed, it has been reported that in cytokine-stimulated CH, NO sustains nuclear translocation of NF-κB, maintaining the NF-κB-dependent transcription persistently activated.[52] This may be the mechanism through which NO promotes cartilage degradation. In this way, NO may promote the expression of proteinases (ie, MMPs) responsible for the degradation of the extracellular matrix. Indeed, the selective inhibition of NF-κB blocks inflammatory bone destruction.[53] Our results show that low doses of PEA (pg/mL) reduced NO formation in TNFα-stimulated CH (Fig. 4). The PEA effect on NO production seems to be in agreement with Mejerink et al., who reported comparable results by other anti-inflammatory NAE including DHEA.[54] Moreover, Mbvundula et al. showed that a synthetic cannabinoid is more potent in inhibiting IL-1a-induced NO production in bovine articular CH than the endogenous N-arachidonoylethanolamine or anandamide. It may be attributed to its readily metabolization by the fatty acid amide hydrolase. In contrast, we found that 2AG significantly increases NO production compared to untreated CH (Fig. 6). 2AG may also be metabolized via COX2 pathway, leading to the formation of pro-inflammatory PG (67). Thus, PEA might appear as a cartilage protective agent by abrogating cartilage matrix degradation through its ability to inhibit NO production. However, further studies are required to elucidate the mechanisms by which this occurs, for example by involving PEA antagonist receptors or FAAH inhibitors. At last, since it is well documented the PUFA involvement in inflammatory context, the cell medium of untreated and TNFα-treated CH was also analyzed for their lipid content. Although previous studies support the role of PUFA in modifying OA severity, data on the effect of TNFα on these lipid precursors are still missing. Here, we showed a clear reduction of all secreted PUFA, both ω6 and ω3, by CH under the inflammatory stimulus (Fig. 7). In this case, all considered treatments were not able to revert the TNFα downregulation. In contrast, no significant differences were displayed for PUFA derivatives (PGD2 and PGF2α) and NAE (PEA, SEA, DHEA) in both untreated and treated CH media, indicating that these lipids were not influenced by the different treatments including TNFα.

Conclusions

A partial lipid content of the secretome from BMSC, ASC, and DF was investigated and a partial bioactive lipid profile has been defined, giving evidence of differences between CM and EV. In our opinion, the identification of key ingredients, including lipids, of MSC and DF secretome, that may be involved in its therapeutic action, could be pivotal for investigating its clinical potential, defining quality control criteria, and allowing future priming approaches in order to improve the efficacy of MSC-based therapies, even with allogeneic products. In the last years, the protein and miRNA content of cell secretome has been extensively investigated, while lipid profiling is still far from complete. Here, 9 lipid compounds were quantified in MSC- and DF-derived secretome. The lipid content was more abundant in almost all MSC-CM and DF-CM rather than paired MSC- and DF-derived EV with a lower degree of homogeneity in CM rather than EV preparations. Considering a possible future clinical application in OA management, we evaluated the in vitro effect of 2AG and PEA, at the concentrations quantified in ASC-CM, in a cellular model of OA. A possible protective effect of PEA and a pro-inflammatory activity and/or lack of effectiveness of 2AG in counteracting TNFα CH stimulation has been shown. As a proof of principle, our findings might support an implication of these bioactive lipids and their related pathways in the OA scenario suggesting a future use of these cell-free products as an innovative therapeutic approach. However, future studies are required considering more complex systems, including organoids or 3D models and/or osteochondral explants.

Funding

The PhD student Sara Casati was supported by the PhD program in Experimental Medicine of the University of Milan, Milan. This research was partly funded by the Italian Ministry of Health (Ricerca Corrente L1038 of IRCCS Istituto Ortopedico Galeazzi).

Conflict of Interest

The authors declared no potential conflicts of interest.

Author Contributions

Conceptualization: S.C., G.C., S.N., A.T.B.; Methodology: S.C.,G.C.,S.N.;Validation:S.C.,E.D.M.;Formalanalysis:S.C.; Investigation: S.C.; Resources: M.O., A.T.B.; Writing: S.C.; Review & Editing: S.C., G.C., S.N.; Visualization: S.C.; Supervision: M.O., A.T.B.; Funding acquisition: M.O., A.T.B.

Data Availability

The data underlying this article will be shared on reasonable request to the corresponding author.

Supplementary Material

Supplementary material is available at *Stem Cells Translational Medicine* online.

References

1. Yang K, Han X. Lipidomics: techniques, applications, and outcomes related to biomedical sciences. *Trends Biochem Sci*. 2016;41(11):954-969. https://doi.org/10.1016/j.tibs.2016.08.010
2. Garc JC, Peris-Díaz MD, Donato MT. A lipidomic cell-based assay for studying drug-induced phospholipidosis and steatosis. *Electrophoresis*. 2017;38:2331-2340.
3. Lydic TA, Goo YH. Lipidomics unveils the complexity of the lipidome in metabolic diseases. *Clin Trans Med*. 2018;7:4.
4. Fahy E, Subramaniam S, Brown HA, et al. A comprehensive classification system for lipids. *J Lipid Res*. 2005;46:839-61.
5. Casati S, Giannasi C, Niada S, Bergamaschi RF, Orioli M, Brini AT. Bioactive lipids in MSCs biology: state of the art and role in inflammation. *Int J Mol Sci*. 2021;22:1481.

6. Van Niel G, D'Angelo G, Raposo G. Shedding light on the cell biology of extracellular vesicles. *Nat Rev Mol Cell Biol*. 2018;19(4):213-228. https://doi.org/10.1038/nrm.2017.125
7. Daneshmandi L, Shah S, Jafari T, Bhattacharjee M, Momah D, Saveh-Shemshaki N, et al. Emergence of the stem cell secretome in regenerative engineering. *Trends Biotechnol*. 2020;38(12):1373-1384. https://doi.org/10.1016/j.tibtech.2020.04.013
8. Abbasi-Malati Z, Roushandeh AM, Kuwahara Y, Roudkenar MH. Mesenchymal stem cells on horizon: a new arsenal of therapeutic agents. *Stem Cell Rev Rep*. 2018;14(4):484-499.
9. Vasandan AB, Jahnavi S, Shashank C, et al. Human mesenchymal stem cells program macrophage plasticity by altering their metabolic status via a PGE_2-dependent mechanism. *Sci Rep*. 2016;6(December):1-17.
10. Ichim TE, Heeron PO, Kesari S. Fibroblasts as a practical alternative to mesenchymal stem cells. *J Transl Med*. 2018;16:1-9. https://doi.org/10.1186/s12967-018-1536-1
11. Nilforoushzadeh MA, Reza H, Ashtiani A, et al. Dermal fibroblast cells: biology and function in skin regeneration. *J Skin Stem Cell*. 2017;4(2):e69080.
12. Niada S, Giannasi C, Gualerzi A, Banfi G, Brini AT. Differential proteomic analysis predicts appropriate applications for the secretome of adipose-derived mesenchymal stem/stromal cells and dermal fibroblasts. *Stem Cells Int*. 2018;2018:11.
13. Carlomagno C, Giannasi C, Niada S, Bedoni M. Raman fingerprint of extracellular vesicles and conditioned media for the reproducibility assessment of cell-free therapeutics. *Front Bioeng Biotechnol*. 2021;9(April):1-9.
14. Niada S, Giannasi C, Magagnotti C, Andolfo A, Brini T. Proteomic analysis of extracellular vesicles and conditioned medium from human adipose-derived stem/stromal cells and dermal fibroblasts. *J Proteomics*. 2021;232:104069. https://doi.org/10.1016/j.jprot.2020.104069
15. Shi Y, Wang Y, Li Q, Liu K, Hou J, Shao C, et al. Immunoregulatory mechanisms of mesenchymal stem and stromal cells in inflammatory diseases. *Nat Rev Nephrol*. 2018;14(8):493-507. https://doi.org/10.1038/s41581-018-0023-5
16. Eleuteri S, Fierabracci A. Insights into the secretome of mesenchymal stem cells and its potential applications. *Int J Mol Sci*. 2019;20(18):4597.
17. Niada S, Giannasi C, Gomarasca M, Stanco D, Casati S, Brini AT. Adipose-derived stromal cell secretome reduces TNFα-induced hypertrophy and catabolic markers in primary human articular chondrocytes. *Stem Cell Res*. 2019;38(March):101463. https://doi.org/10.1016/j.scr.2019.101463
18. Giannasi C, Niada S, Magagnotti C, et al. Comparison of two ASC-derived therapeutics in an in vitro OA model: secretome versus extracellular vesicles. *Stem Cell Res Ther*. 2020;5:1-15.
19. Casati S, Giannasi C, Minoli M, et al. Quantitative lipidomic analysis of osteosarcoma cell-derived products by UHPLC-MS/MS. *Biomolecules*. 2020;10:13021-13022. https://doi.org/10.3390/biom10091302
20. Laganà M, Arrigoni C, Lopa S, et al. Characterization of articular chondrocytes isolated from 211 osteoarthritic patients. *Cell Tissue Bank*. 2014;15(1):59-66. doi:10.1007/s10561-013-9371-3
21. Gualerzi A, Niada S, Giannasi C, et al. Raman spectroscopy uncovers biochemical tissue-related features of extracellular vesicles from mesenchymal stromal cells. *Sci Rep*. 2017;7(1):1-11. https://doi.org/10.1038/s41598-017-10448-1
22. Caron M, Emans P, Coolsen M, et al. Redifferentiation of dedifferentiated human articular chondrocytes: comparison of 2D and 3D cultures. *Osteoarthr Cart*. 2012;20(10):1170-1178.
23. Goldrin M. Human chondrocyte cultures as models of cartilage-specific gene regulation. *Methods Mol Med*. 2005;107:69-95.
24. Westacott C, Barakat A, Wood L, et al. Tumor necrosis factor alpha can contribute to focal loss of cartilage in osteoarthritis. *Osteoarthr Cart*. 2000;8(3):213-221.
25. Niada S, Giannasi C, Gomarasca M, Stanco D, Casati S, Teresa A. Adipose-derived stromal cell secretome reduces TNFα-induced hypertrophy and catabolic markers in primary human articular chondrocytes. *Stem Cell Res*. 2019;38(May):101463. https://doi.org/10.1016/j.scr.2019.101463
26. Fitzsimmons REB, Mazurek MS, Soos A, Simmons CA. Review article mesenchymal stromal/stem cells in regenerative medicine and tissue engineering. *Stem Cells Int*. 2018;2018:8031718.
27. Giannasi C, Niada S, Morte ED, et al. Towards secretome standardization: identifying key ingredients of MSC-derived therapeutic cocktail. *Stem Cells Int*. 2021;2021:3086122.
28. Tang Y, Huang Y, Zheng LEI, Qin S, Xu X, An T. Comparison of isolation methods of exosomes and exosomal RNA from cell culture medium and serum. *Int J Mol Med*. 2017; 40:834-844.
29. Takov K, Yellon DM, Davidson SM, Takov K, Yellon DM, Comparison SMD. Comparison of small extracellular vesicles isolated from plasma by ultracentrifugation or size-exclusion chromatography: yield, purity and functional potential. *J Extracell Vesicles*. 2019;8(1):1560809. https://doi.org/10.1080/20013078.2018.1560809
30. D'Arrigo D, Roffi A, Cucchiarini M, et al. Secretome and extracellular vesicles as new biological therapies for knee osteoarthritis: a systematic review. *J Clin Med* 2019;8(11):1867.
31. Mancuso P, Raman S, Glynn A, Barry F, Murphy JM. Mesenchymal stem cell therapy for osteoarthritis: the critical role of the cell secretome. *Front Bioeng Biotechnol*. 2019;7(January):1-9.
32. Vergauwen G, Dhond B, Van Deun J, De Smedt E, Berx G, Timmerm E, et al. Confounding factors of ultrafiltration and protein analysis in extracellular vesicle research. *Sci Rep*. 2017;7(1):2704.
33. Witkamp R. Fatty acids, endocannabinoids and inflammation. *Eur J Pharmacol*. 2016;785:96-107. https://doi.org/10.1016/j.ejphar.2015.08.051
34. Barrie N, Manolios N. The endocannabinoid system in pain and inflammation: its relevance to rheumatic disease. *Eur J Rheumatol*. 2017;1(13):210-218.
35. Ioan-Facsinay A, Kloppenburg M. Bioactive lipids in osteoarthritis: risk or benefit? *Curr Opin Rheumatol*. 2018;30(1):108-113.
36. Pousinis P, Gowler PRW, Burston JJ, Ortori CA, Chapman V, Barrett DA. Lipidomic identification of plasma lipids associated with pain behaviour and pathology in a mouse model of osteoarthritis. *Metabolomics*. 2020;16(3):1-13. https://doi.org/10.1007/s11306-020-01652-8
37. Oppedisano F, Bulotta RM, Maiuolo J, et al. Review article. The role of nutraceuticals in osteoarthritis prevention and treatment: focus on n-3 PUFAs. *Oxid Med Cell Longev*. 2021;2021:4878562.
38. Mehler SJ, May LR, King C, Harris WS, Shah Z. A prospective, randomized, double blind, placebo-controlled evaluation of the effects of eicosapentaenoic acid and docosahexaenoic acid on the clinical signs and erythrocyte membrane polyunsaturated fatty acid concentrations in dogs with osteoarthritis. *Prostaglandins Leukot Essent Fat Acids*. 2016;109:1-7. https://doi.org/10.1016/j.plefa.2016.03.015
39. Van de Vyver A, Clockaerts S, Van de Lest CHA, et al. Synovial fluid fatty acid profiles differ between osteoarthritis and healthy patients. *Cartilage*. 2020;11(4):473-478. doi:10.1177/1947603518798891
40. La Porta C, Bura SA, Negrete R, Maldonado R. Involvement of the endocannabinoid system in osteoarthritis pain. *Eur J Neurosci*. 2014;39:485-500.
41. La Porta C, Bura SA, Llorente-Onaindia J, Pastor A, Navarrete F. Role of the endocannabinoid system in the emotional manifestations of osteoarthritis pain. *Pain*. 2015;156(10):2001-2012. https://doi.org/10.1097/j.pain.0000000000000260
42. Gabrielsson L, Gouveia-Figueira S, Haggstrom J, Alhouayek M, Fowler C. The anti-inflammatory compound palmitoylethanolamide inhibits prostaglandin and hydroxyeicosatetraenoic acid production by a macrophage cell line. *Pharmacol Res Perspect*. 2017;5(2):e00300.
43. Tchetina EV, Di Battista BJ, Zukor DJ, Antoniou J, Poole AR. Research article. Prostaglandin PGE 2 at very low concentrations suppresses collagen cleavage in cultured human osteoarthritic articular cartilage: this involves a decrease in expression of

proinflammatory genes, collagenases and COL10A1, a gene linked to chondrocyte hypertrophy. *Arthritis Res Ther*. 2007;9(4):1-9.
44. Roman-Blas J, Jimenez M. NF-κB as a potential therapeutic target in osteoarthritis and rheumatoid arthritis. *Osteoarthr Cartil*. 2006;14:839-848.
45. Esposito G, Capoccia E, Turco F, Palumbo I, Lu J, Steardo A, et al. Palmitoylethanolamide improves colon inflammation through an enteric glia/toll like receptor 4-dependent PPAR-α activation. *Gut*. 2014; 63:1300-1312.
46. Agostino GD, La Rana G, Russo R, Sasso O, Iacono A, Esposito E, et al. Central administration of palmitoylethanolamide reduces hyperalgesia in mice via inhibition of NF-κB nuclear signalling in dorsal root ganglia. *Eur J Pharmacol*. 2009;613(1-3):54-59. https://doi.org/10.1016/j.ejphar.2009.04.022
47. Romano A, Romano A, Friuli M, Del Coco L, Longo S, Vergara D, et al. Chronic oleoylethanolamide treatment decreases hepatic triacylglycerol level in rat liver by a PPARγ/SREBP-mediated suppression of fatty acid and triacylglycerol synthesis. *Nutrients*. 2021;13(2):394.
48. Amin AR, Abramson SB. The role of nitric oxide in articular cartilage breakdown in osteoarthritis. *Curr Opin Rheumatol*. 1998;10:263-268.
49. Mendes AF, Carvalho AP, Caramona MM, Lopes MC. Role of nitric oxide in the activation of NF-κB, AP-1 and NOS II expression in articular chondrocytes. *Inflamm Res*. 2002;51: 369-375.
50. Abramson SB. Osteoarthritis and nitric oxide. *Osteoarthr Cartil*. 2008;16(Suppl 2):S15-20.
51. Leonidou A, Lepetsos P, Mintzas M, et al. Inducible nitric oxide synthase as a target for osteoarthritis treatment. *Expert Opin Ther Targets*. 2018;22(4):299-318. https://doi.org/10.1080/14728222.2018.1448062
52. Clancy RM, Gomez PF, Abramson SB. Nitric oxide sustains nuclear factor kappaB activation in cytokine-stimulated chondrocytes. *Osteoarthr Cartil*. 2004;552-558.
53. Jimi E, Aoki K, Saito H, et al. Selective inhibition of NF-κB blocks osteoclastogenesis and prevents inflammatory bone destruction in vivo. *Nat Med*. 2004;10(6):617-624.
54. Meijerink J, Plastina P, Vincken J, et al. The ethanolamide metabolite of DHA, docosahexaenoylethanolamine, shows immunomodulating effects in mouse peritoneal and RAW264. 7 macrophages: evidence for a new link between fish oil and inflammation. *Br J Nutr*. 2011;105:1798-1807. https://doi.org/10.1017/S0007114510005635